

Fragmentation instability in aggregating systems

Arturo Berrones-Santos^{1,*}, Luis Benavides-Vázquez², Elisa Schaeffer¹, and Javier Almaguer³

¹Posgrado en Ingeniería de Sistemas, Facultad de de Ingeniería Mecánica y Eléctrica, Universidad Autónoma de Nuevo León, San Nicolás de los Garza, N.L., México

²School of Engineering and Sciences, Tecnológico de Monterrey, Monterrey, N.L., Mexico

³Doctorado en Ciencias con Orientación en Matemáticas, Facultad de Ciencias Físico Matemáticas, Universidad Autónoma de Nuevo León, San Nicolás de los Garza, N.L., México

*Corresponding author: arturo.berronesn@uanl.edu.mx

March 14, 2022

Abstract

The inclusion of a fragmentation mechanism in population balance equations introduces complex interactions that make the analytical or even computational treatment much more difficult than for the pure aggregation case. This is specially true when variable sized fragments are allowed, because of the exponential growth in fragments size combinations with the number of monomers in the exchanges. In this contribution we present a new model that incorporates an instability threshold in the clusters, which induces arbitrary losses or gains of particles by fracture with a substantial simplification of the combinatorics of the process. The model exhibits two different regimes.

1 Introduction

Despite that aggregation processes have been under study since the 1910's after the seminal work by Smoluchowski [1], the understanding of the phenomena that emerge from these processes is far to be complete. For instance, only very recently has been formally proved that the gelation without fracture observed not only in colloids [2] but also in the form of a “giant component” present in such disparate systems like stars [3] or social networks [4, 30] is indeed a thermodynamic phase transition [6]. The inclusion of fragmentation mechanisms only increases the number of interesting behaviors like the emergence of stationary states with unusual statistical properties [7, 8], which are relevant for applications like biological networks [9, 10], econophysics [11] or chemical and

physical systems out of equilibrium [32]. The classical framework to deal with aggregation-fragmentation processes is given by the generalized Smoluchowski rate equation [8],

$$\begin{aligned} \frac{d\rho_n}{dt} = & \frac{1}{2} \sum_{i+j=n} [K_{i,j}\rho_i\rho_j - F_{i,j}\rho_{i+j}] \\ & - \sum_{j=1}^{\infty} [K_{n,j}\rho_n\rho_j - F_{n,j}\rho_{n+j}]. \end{aligned} \quad (1)$$

Equation (1) describes the evolution of the density of clusters with size n , ρ_n , in terms of the aggregation kernel $K_{i,j}$ (which gives the aggregation reaction rate of an i -mer with a j -mer) and the fragmentation kernel $F_{i,j}$ (models the break-up of a $(i+j)$ -mer into an i -mer and a j -mer). It should be remarked that Eq. (1) is a mean field description, which gives no information regarding spatial fluctuations. The study of the mathematical properties of Eq. (1) is an active research area [12–14], however the combinatorics introduced by the fragmentation terms make the analytical treatment very difficult even with simple kernel structures. From a computational standpoint, the presence of fragmentation makes the numerical solution of Eq. (1) also in general intractable, because the evident exponential computing times unless the fracture exchanges are in some way limited. The most studied special case has been the situation with single particle fractures, like in the “one-chip” or in the Becker-Döring models [7, 8, 15]. Very recently it has been also put forward a quite general setup in which the fragmentation is complete, that is, it results in a full decomposition into monomers [21]. Under this assumption, a thorough analytical and numerical characterization of a variety of aggregation mechanisms is given in [21].

In the present work we introduce a new model that allows fragments with an arbitrary number of monomers but with simple combinatorics. The model is inspired in processes in which “large” clusters behave in a different way than “small” clusters. Our original motivation was the jar test apparatus for wastewater treatment reported in [32], for which some of the authors of the present contribution developed a cellular automaton model. A mean field description for processes with the same general microscopic properties is the purpose of the present contribution. In the jar test apparatus, a transition from gel states to stationary particle size distributions in which very large clusters are dominant is observed. The transition is induced by instabilities in the large clusters, controlled by an external energy input. Similar situations may also arise for instance in socio-economic systems, where large organizations can fracture into smaller ones but also can acquire parts of other large organizations or entirely absorb small ones, while small organizations are able to grow only by aggregation of simple units of capital or shares. In these kind of instances, there is a natural asymmetry by which large clusters behave like hubs for small clusters but also display a tipping point after which they become intrinsically unstable. There is a number of applications in which this emergence of asymmetry after

a threshold is reported [16–19]. In first instance our model can be adapted to these situations and in consequence an open system in which mass conservation can be violated is tacitly assumed. The closed system version of the model will be reported elsewhere. The statistical properties of the stationary regimes can be derived from a characteristic function in a number of general cases (for a discussion of the use of characteristic functions in statistical physics, specially the technique based on the Z-function, which is the one followed by us in our analytical description below, see for instance [28]).

2 Instability threshold aggregation-fragmentation model

The basic feature of our model is the introduction of a global instability threshold, \bar{h} . This can be interpreted as a physical constant that acts on all of the clusters in the system, similar to those used in models for sandpiles [16], earthquakes [18, 19] and fracture of materials [17]. To our knowledge, our model is the first that adds such a mechanism in aggregation-fragmentation processes modeled by Smoluchowski-type rate equations. Our basic concept is that clusters with a number of particles above \bar{h} became unstable and can fracture with a constant probability. A fracture gives rise to two clusters, one of which is barely stable with size \bar{h} . From a microscopic level, one may say that the original cluster has transferred its “excess” particles. Fragments from an originally large cluster can be absorbed by other large clusters above \bar{h} . This introduces an asymmetry between clusters below and above the instability threshold, which implies an open system in which there can be a flux of mass out of the system to a gel state. Interestingly, as shown below, stationary states can still emerge despite this fact. The gel regime on the other hand, is attained in a finite time.

The inclusion of the parameter \bar{h} permits a radical simplification of the fragmentation terms of the Smoluchowski-type model without losing the exchanges resulting in large fragments present in the general case, at the cost of the need for two regimes,

$$\begin{aligned}
 & n = i + j > \bar{h} : & (2) \\
 \frac{d\rho_n}{dt} &= \frac{1}{2} \sum_{i+j=n} K_{i,j} \rho_i \rho_j - \sum_{j=1}^{\infty} K_{n,j} \rho_n \rho_j - \frac{F}{2} \rho_n + F \rho_{n+\bar{h}}. \\
 & n = i + j \leq \bar{h} : \\
 \frac{d\rho_n}{dt} &= \frac{1}{2} \sum_{i+j=n} K_{i,j} \rho_i \rho_j - \sum_{j=1}^{\infty} K_{n,j} \rho_n \rho_j.
 \end{aligned}$$

The possibly exponentially growing combinatorics obviously persists in the aggregation terms, but these are tractable for some general kernels $K_{i,j}$ due to the separability in the ρ 's.

3 Related recent literature

A number of advances to tackle generalizations of population balance models beyond constant kernels and with spontaneous fragmentation have been very recently put forward [21–24]. The main difference of the setup given by the expressions (2) with respect to these other recent approaches is the discontinuous nature of the spontaneous fragmentation probability induced by an instability threshold, which can lead to states with a population dominated by very large fragments or can go to a gel phase. For instance, in the already mentioned work [21], analytical solutions under collisional kernels are given, supporting aggregation and spontaneous and collisional fragmentation. This model clearly represents a substantial step beyond the classical theoretical results under simple aggregation and fragmentation mechanisms. However, the fragmentation is subjected to a regularity condition that limits the process to be “complete”, that is, it results in a division in the basic constituent monomers. This is suitable for cases in which small monomers or debris dominate the particle size distribution. An application to particle size distributions in Saturn’s rings is given of this collisional model is given in [22] and in [23] a numerical approach for such type of models with collisional fragmentation is given. In [24], by writing the population rate equation in integral form, the authors find exact solutions by the so called homotopy method. The approach is quite general and admits spontaneous fragmentation by assuming continuous fragmentation rates. It would be an interesting future research direction to investigate the possible implementation of this approach to our discontinuous setup.

From a computational standpoint, fast algorithms for the direct numerical solution of the rate equations have been recently proposed. In particular [25] is capable to deal with very general kernel structures by a low-rank transformation at the cost of ignoring the tails of the particle size distribution. This at first instance seems not well suited for our model in which as already mentioned, the existence of states with large particle sizes is of interest. It may however be fruitfully adapted to the study of some of our stationary regimes. In its standard formulation this fast algorithm (and other recent proposals like [26]) does not consider fragmentation, so generalizations are in order to explore our instability model by direct numerical solution. We have proposed a cellular automaton like an at first instance best suited numerical framework for our model. Our original motivation for the associated cellular automaton model has been a waste water treatment experiment in a jar test apparatus in which by the injection of external energy, agitation favours the large flock formation, but when the flocks exceed a certain threshold, instabilities emerge that can cause fracture [32]. Other application that in our opinion is worth to be explored in the future is in the fragmentation of social networks. There is an increasing body of evidence that in networks of individuals or of social organizations, the fragmentation is dominated by tipping points and not by the continuous fragmentation rates usually studied in population balance approaches. See for instance [27] for discussions of fragmentation in social contexts. Community formation processes have been extensively studied by complex networks models

[28–30], but the study of models for community fragmentation is still scarce [31]. Our Smoluchowski-type setup can be a useful mean field description of these social networks processes.

4 Analysis under different aggregation kernels

4.1 Constant aggregation rate

With constant aggregation kernel, the model reduces to

$$\begin{aligned}
 n = i + j > \bar{h} : \quad (3) \\
 \frac{d\rho_n}{dt} = \frac{1}{2}K \sum_{j=1}^{n-1} \rho_j \rho_{n-j} - K \sum_{j=1}^{\infty} \rho_n \rho_j - \frac{F}{2}\rho_n + F\rho_{n+\bar{h}}. \\
 n = i + j \leq \bar{h} : \\
 \frac{d\rho_n}{dt} = \frac{1}{2}K \sum_{j=1}^{n-1} \rho_j \rho_{n-j} - K \sum_{j=1}^{\infty} \rho_n \rho_j
 \end{aligned}$$

The Z-transform (characteristic function) $\hat{\rho}(z) = \sum_{n=1}^{\infty} \rho_n z^{-n}$ of the model (3) reads

$$\frac{d\hat{\rho}(z, t)}{dt} = \frac{K}{2}\hat{\rho}^2(z, t) - \hat{\rho}(z, t) \left[K\hat{\rho}(1, t) + \frac{F}{2}(1 - 2z^{\bar{h}}) \right] - F \sum_{j=1}^{\bar{h}-1} \rho_j z^{\bar{h}-j} \quad (4)$$

which admits stationary solutions,

$$\hat{\rho}(z) = \hat{\rho}(1) + \frac{F}{2K}(1 - 2z^{\bar{h}}) \pm \frac{1}{2} \sqrt{\left[2\hat{\rho}(1) + \frac{F}{K}(1 - 2z^{\bar{h}}) \right]^2 + 8 \left(\frac{F}{K} \right) \sum_{j=1}^{\bar{h}-1} \rho_j z^{\bar{h}-j}}, \quad (5)$$

where

$$\hat{\rho}(1) = \frac{F}{2K} \pm \frac{1}{2} \sqrt{\left(\frac{F}{K} \right)^2 - 8 \left(\frac{F}{K} \right) \sum_{j=1}^{\bar{h}-1} \rho_j} \quad (6)$$

is the total number of clusters in the system. In the stationary regime, $1/\hat{\rho}(1)$ is a normalization factor and the moments of the stationary cluster size distribution follow from the derivatives of the characteristic function. For instance, $\langle n \rangle = \frac{-1}{\hat{\rho}(1)} \frac{d\hat{\rho}}{dz} \Big|_{z=1}$ and $\langle n(n+1) \rangle = \frac{1}{\hat{\rho}(1)} \frac{d^2\hat{\rho}}{dz^2} \Big|_{z=1}$. By taking derivatives in equation (4), a closed system for the first two moments in terms of the normalization factor

is obtained,

$$\begin{aligned}
-K\hat{\rho}(1)\langle n\rangle + \langle n\rangle \left[K\hat{\rho}(1) - \frac{F}{2} \right] + F\bar{h} - \frac{F}{\hat{\rho}(1)} \sum_{j=1}^{\bar{h}-1} (\bar{h}-j)\rho_j &= 0 \quad (7) \\
K\hat{\rho}(1)\langle n(n+1)\rangle + K\hat{\rho}(1)\langle n\rangle^2 - 2F\bar{h}\langle n\rangle \\
-\langle n(n+1)\rangle \left[K\hat{\rho}(1) - \frac{F}{2} \right] + [F\bar{h}(\bar{h}-1)] \\
-\frac{F}{\hat{\rho}(1)} \sum_{j=1}^{\bar{h}-1} (\bar{h}-j)(\bar{h}-j-1)\rho_j &= 0,
\end{aligned}$$

from which,

$$\frac{1}{2}\langle n\rangle = \bar{h} - \frac{1}{\hat{\rho}(1)} \sum_{j=1}^{\bar{h}-1} (\bar{h}-j)\rho_j, \quad (8)$$

$$\frac{1}{2}\langle n(n+1)\rangle = 2\langle n\rangle\bar{h} - \frac{K}{F}\hat{\rho}(1)\langle n\rangle^2 - \bar{h}(\bar{h}-1) + \frac{1}{\hat{\rho}(1)} \sum_{j=1}^{\bar{h}-1} (\bar{h}-j)(\bar{h}-j-1)\rho_j.$$

By introducing the definitions, $\alpha \equiv \frac{1}{\hat{\rho}(1)} \sum_{j=1}^{\bar{h}-1} \rho_j$, $\beta \equiv \frac{1}{\hat{\rho}(1)} \sum_{j=1}^{\bar{h}-1} j\rho_j$ and $\gamma \equiv \frac{1}{\hat{\rho}(1)} \sum_{j=1}^{\bar{h}-1} j^2\rho_j$ follows that,

$$\begin{aligned}
\langle n\rangle &= \frac{\bar{h}(1-\alpha)}{\frac{1}{2}-\beta}, \quad (9) \\
\langle n^2\rangle(1-2\gamma) &= \langle n\rangle(4\bar{h}-1) - \frac{2K}{F}\hat{\rho}(1)\langle n\rangle^2 - 2\bar{h}(\bar{h}-1) \\
&+ 2(\alpha\bar{h}^2 - 2\beta\bar{h}\langle n\rangle - \alpha\bar{h} + \beta\langle n\rangle),
\end{aligned}$$

so the first two moments of the stationary distribution are well defined under the conditions $0 < \alpha < 1$, $0 < \beta < 1/2$, $\gamma > 1/2$. The mean grows linearly with \bar{h} and the variance is parabolic in \bar{h} . At small but non zero (F/K), mean and variance are large and diverge in the limit (F/K) $\rightarrow 0$ while $\hat{\rho}(1) \rightarrow 0$, which corresponds to the limit $\beta \rightarrow 1/2$. This kind of stationary state is attained in finite time. To see this, consider (F/K) $\ll 1$. From Eq.(6) follows that,

$$\frac{F}{K} = \frac{1}{1 - \frac{2}{\alpha} \sum_{j=1}^{\bar{h}-1} \rho_j} \quad (10)$$

Note also that at (F/K) $\ll 1$ the sum $\sum_{j=1}^{\bar{h}-1} \rho_j \ll \hat{\rho}(1)$, so

$$\frac{d\hat{\rho}(1,t)}{dt} = -\frac{K}{2}\hat{\rho}^2(1,t) + \frac{F}{2}\hat{\rho}(1,t), \quad (11)$$

which leads to

$$\hat{\rho}(1,t) = \frac{F}{K[1 - e^{-(\frac{F}{2})t}]} \quad (12)$$

Therefore, the system displays a stationary state with large mean and variance at $(F/K) \ll 1$ and above a characteristic time $t_c \approx \frac{2}{F}$. This behavior is absent in the pure aggregation model with constant kernel, where a gelation transition occurs at infinite time.

4.2 Additive and multiplicative aggregation rate

For aggregation kernels of the form $K_{i,j} = K(i+j)/2$ and $K_{i,j} = Kij$, where K is some positive constant, the resulting system of equations for the moments is not closed, but however some important features of the stationary states can be derived.

In the additive case,

$$\begin{aligned} n = i + j > \bar{h} : \quad (13) \\ \frac{\partial \rho_n}{\partial t} = \frac{Kn}{4} \sum_{j=1}^{n-1} \rho_j \rho_{n-j} - \frac{Kn\rho_n}{2} \sum_{j=1}^{\infty} \rho_j - \frac{K\rho_n}{2} \sum_{j=1}^{\infty} j\rho_j - \frac{F}{2}\rho_n + F\rho_{n+\bar{h}}. \\ n = i + j \leq \bar{h} : \\ \frac{\partial \rho_n}{\partial t} = \frac{K}{4} \sum_{i+j=n} (i+j)\rho_i\rho_j - \frac{K}{2} \sum_{j=1}^{\infty} (n+j)\rho_n\rho_j. \end{aligned}$$

and the Z-transform of the model reads,

$$\begin{aligned} \frac{\partial \hat{\rho}(z, t)}{\partial t} = -\frac{K}{2} z \hat{\rho}(z, t) \frac{\partial \hat{\rho}(z, t)}{\partial z} + \frac{K}{2} z \hat{\rho}(1, t) \frac{\partial \hat{\rho}(z, t)}{\partial z} - \frac{K}{2} M_1(t) \hat{\rho}(z, t) \quad (14) \\ - \frac{F}{2} (1 - 2z^{\bar{h}}) \hat{\rho}(z, t) - F \sum_{j=1}^{\bar{h}-1} \rho_j z^{\bar{h}-j}, \end{aligned}$$

where $M_1(t) \equiv \sum_{j=1}^{\infty} j\rho_j$. If the definition for $\langle n \rangle$ is introduced in (14), it turns out that there exists a stationary state in which

$$\langle n \rangle = \frac{F}{K} \left[1 - 2 \left(\frac{\sum_{j=1}^{\bar{h}-1} \rho_j}{\hat{\rho}(1)} \right) \right], \quad (15)$$

given the condition $\hat{\rho}(1) > 2 \sum_{j=1}^{\bar{h}-1} \rho_j$.

The product aggregation kernel $K_{i,j} = Kij$ leads to

$$\begin{aligned} n = i + j > \bar{h} : \quad (16) \\ \frac{d\rho_n}{dt} = \frac{1}{2} \sum_{i+j=n} ij\rho_i\rho_j - \sum_{j=1}^{\infty} nj\rho_n\rho_j - \frac{F}{2}\rho_n + F\rho_{n+\bar{h}}. \\ n = i + j \leq \bar{h} : \\ \frac{d\rho_n}{dt} = \frac{1}{2} \sum_{i+j=n} ij\rho_i\rho_j - \sum_{j=1}^{\infty} nj\rho_n\rho_j, \end{aligned}$$

with the associated characteristic function,

$$\begin{aligned} \frac{\partial \hat{\rho}(z, t)}{\partial t} = & \frac{K}{2} z^2 \left[\frac{\partial \hat{\rho}(z, t)}{\partial z} \right]^2 + K z M_1(t) \frac{\partial \hat{\rho}(z, t)}{\partial z} \\ & - \frac{F}{2} (1 - 2z^{\bar{h}}) \hat{\rho}(z, t) - F \sum_{j=1}^{\bar{h}-1} \rho_j z^{\bar{h}-j} \end{aligned} \quad (17)$$

The pure aggregation case ($F = 0$) has been widely studied and display a number of interesting behaviors [15]. In the presence of fragmentation, stationary states emerge. To proceed substitute the definition for $\langle n \rangle$ into equation (17), giving

$$\langle n \rangle = \sqrt{\frac{F \left[\sum_{j=1}^{\bar{h}-1} \rho_j - \frac{1}{2} \hat{\rho}(1) \right]}{K \hat{\rho}(1) \left[\frac{1}{2} \hat{\rho}(1) - 1 \right]}} \quad (18)$$

so there is a stationary state in which all the mass is concentrated in a finite number of clusters. The total number of clusters is in the interval $2 \leq \hat{\rho}(1) \leq 2(\bar{h} - 1)$.

5 Microscopic justification of the instability threshold: a cellular automaton model

A microscopic counterpart of the constant kernels version of our model can be given in terms of the following cellular automaton (which generalizes a model introduced by Almaguer et al. [32]): consider a n -cell d -dimensional wrap lattice (for example, in a 1-d automaton, the first cell is adjacent with the last cell). The cell coordinates are hence a vector with d elements. A cell is a *neighbor* of another if and only if the coordinates of the two cells differ by exactly one unit in exactly one position.

Each cell i of the lattice has an integer-valued state variable h_i that represents the floc size at that cell. We call the units that form the flocs *particles*. The automaton is initialized by placing uniformly and independently at random a total of m particles in the n cells of the lattice, such that the initial average floc-size is given by $\bar{h} = \frac{m}{n}$. A set of local rules, adapted from those of Almaguer et al. [32], governs the change of each h_i between the current state of the automaton and the next state, in terms of an *aggregation rate* f and a *fragmentation rate* v .

Rule 1: if $h_i \leq \bar{h}$ then, with probability v , cell i *absorbs* the $[\bar{h}] - h_i$ *excess* of each of its neighbors.

Rule 2: if $h_{i,j} > \bar{h}$ then, with probability $f \cdot (1 - v)$, the cell i *absorb* all the particles of all of its neighbors (as in Rule 1); otherwise the cell *transfers* a fraction uniformly at random of its $[\bar{h}] - h_i$ *excess* particles, choosing the receptor cell uniformly at random among its neighbors.

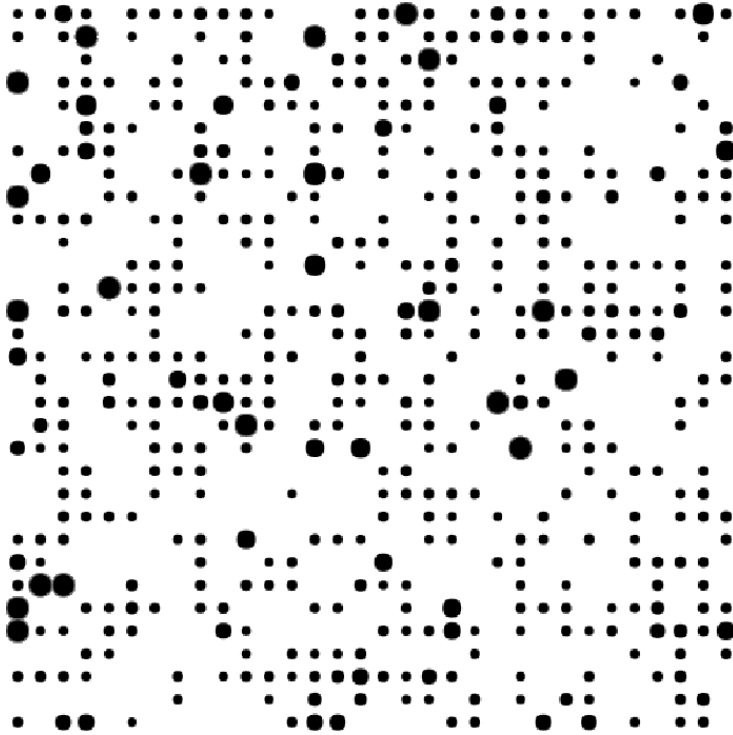


Figure 1: A visualization of a stationary state of a 2-d automaton. The area of each dot is linearly proportional to the floc size of the cell.

First, at each time step, each cell i is processed in a random order. Then, according to the Rules 1 and 2, each cell i updates its receptions or transfers according to the values of the state variables of the cell itself and its neighbors in the present state. An asynchronous update scheme is performed, in such a way that the new state of a cell affects the calculation of states in neighboring cells. At the end of the simulation, the floc-size distribution is obtained from the automaton.

These rules govern local fluctuations on the particle exchange among the flocs in terms of the relative size of each floc at each cell i with respect to the stability *threshold*, the average floc-size \bar{h} . Notice that involves local fluctuations in which mass can be transported by fracture of large clusters to small ones. However, because of the asymmetry in the absorption rates of the neighborhood particles, the mean field description given in 2 is adequate, as argued by the experiments given below.

A visual representation of a typical stationary state of the described 2-d model is given in Figure 1.

The parameter v governs floc *instability*: when $v \rightarrow 1$, only flocs of sizes below or equal to the average are stable. The parameter f , on the other hand,

controls floc *stabilization*: floc growth depends on f when $v < 1$. Therefore the limit $\frac{F}{K} \rightarrow 0$ corresponds to $f \rightarrow 1, v \rightarrow 0$ and the limit $\frac{F}{K} \gg 1$ corresponds to $f \rightarrow 0, v \rightarrow 1$. We now show that this microscopic model displays the average behavior predicted by our Smoluchowski-type model. In the absence of fragmentation, the final state should be given by a gel state. We initialize the automaton starting each cell with a floc of size one. There are n total cells. The parameters are fixed to $f = 1$ (pure aggregation) and $v = 0.001$ (low fragmentation rate, it cannot be equal to zero). The simulation stops when a singular cell contains a floc of size n . Ten replicas of the simulation were executed for dimensions from two to five, from which a stopping criteria for the automaton is defined for each dimension, as explained in [33]. In the same previous work [33] we explain how to calibrate the automaton parameters and in this way obtain a physical time scale corresponding to the automaton discrete steps. In that work the steady state particle distributions of an experimental jar test apparatus with agglomeration and velocity is studied by microscopic images. The parameters are adjusted by statistical tests on the similarity between the automaton and experimentally observed particle size distributions. In that particular application it turned out that 10^6 time steps correspond to 7 minutes of the jar test experiment. For the stationary states is predicted a linear dependency on \bar{h} of the mean and a parabolic dependence on \bar{h} of the variance of the cluster size distribution, like stated by the expressions in (9). More interestingly, these expressions describe a range of size distributions ranging from those in which small clusters dominate to gel-like situations in which the particles tend to concentrate in a small number of very large clusters.

In Figure 2 we show the average floc size at four different values of \bar{h} with the automaton settings $f = 0.1, v = 0.9$. Is clear the linear dependence with \bar{h} predicted by (9). The variance under the same setup is reported in Figure 3, which again is consistent with the behavior predicted by equation (9). A stationary state with large values of mean and variance relative to \bar{h} is on the other hand reported in Figure 4. In this case the parameters of the automaton are given by $f = 0.9, v = 0.1$ which is consistent with the predictions for $\frac{F}{K} \rightarrow 0$. In all cases the reported figures correspond to 10 repetitions for each setup, with 10000 time steps. We have observed that for this number of time steps the particle size distribution is approximately stationary.

6 Conclusion

A new Smoluchowski-type aggregation-fragmentation model has been introduced for which is possible to analytically derive important statistical features. To our knowledge, this is the first Smoluchowski-type model with variable sized fragmentation and instability that is amenable for analytical treatment. For the constant kernels case, a microscopic counterpart has been constructed in terms of a cellular automaton. The simulations are in agreement with the predictions derived from the Smoluchowski-type model. The framework introduced in this work is relevant to applications in which populations of clusters that can

aggregate become unstable at sizes above some threshold. For instance, there is experimental evidence that this might be the case in the removal of heavy metals from wastewater through coagulation and agitation [32]. Other possible application of the model is in social networks, where intuitively is plausible that large communities above some size are more prone to fracture into smaller communities.

Acknowledgement

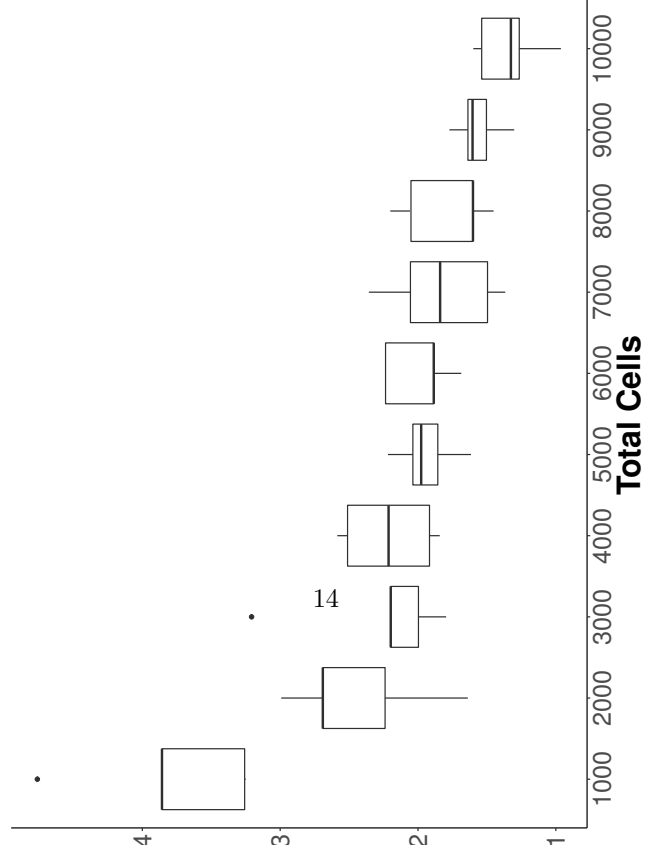
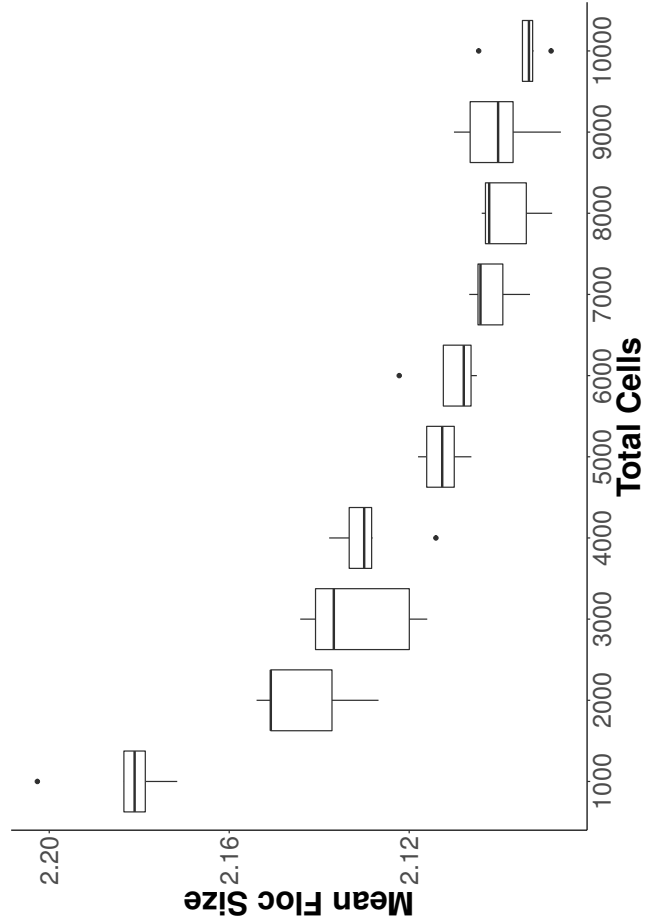
This work was partially supported by supported by UANL-PAICYT under grant IT1807-21 and by CONACYT under grant CB-167651.

References

- [1] Smoluchowski, M. V. (1916). Über Brownsche Molekularbewegung unter Einwirkung äußerer Kräfte und deren Zusammenhang mit der verallgemeinerten Diffusionsgleichung. *Annalen der Physik*, 353(24), 1103-1112.
- [2] Poon, W. C., & Haw, M. D. (1997). Mesoscopic structure formation in colloidal aggregation and gelation. *Advances in Colloid and Interface Science*, 73, 71-126.
- [3] Allen, E. J., & Bastien, P. (1995). On coagulation and the stellar mass spectrum. *The Astrophysical Journal*, 452, 652.
- [4] Kumar, R., Novak, J., & Tomkins, A. (2010). Structure and evolution of online social networks. In *Link mining: models, algorithms, and applications* (pp. 337-357). Springer New York.
- [5] Barabási, A. L. (2016). *Network science*. Cambridge University Press.
- [6] Matsoukas, T. (2015). Statistical thermodynamics of irreversible aggregation: the sol-gel transition. *Scientific reports*, 5.
- [7] Majumdar, S. N., Krishnamurthy, S., & Barma, M. (2000). Nonequilibrium phase transition in a model of diffusion, aggregation, and fragmentation. *Journal of Statistical Physics*, 99(1), 1-29.
- [8] Vigil, R. D. (2009). On equilibrium solutions of aggregation-fragmentation problems. *Journal of colloid and interface science*, 336(2), 642-647.
- [9] Bressloff, P. C. (2016). Aggregation-fragmentation model of vesicular transport in neurons. *Journal of Physics A: Mathematical and Theoretical*, 49(14), 145601.
- [10] Pakdaman, K., Perthame, B., & Salort, D. (2014). Adaptation and fatigue model for neuron networks and large time asymptotics in a nonlinear fragmentation equation. *The Journal of Mathematical Neuroscience*, 4(1), 1-26.

- [11] Chakrabarti, B. K., Chakraborti, A., Chakravarty, S. R., & Chatterjee, A. (2013). *Econophysics of income and wealth distributions*. Cambridge University Press.
- [12] Banasiak, J. (2012) Global classical solutions of coagulation-fragmentation equations with unbounded coagulation rates, *Nonlinear Analysis: Real World Applications* 13 (1) 91–105.
- [13] Banasiak, J., Lamb, W. (2011) Global strict solutions to continuous coagulation-fragmentation equations with strong fragmentation, *Proceedings of the Royal Society of Edinburgh: Section A Mathematics* 141, 465–480.
- [14] Banasiak, J. (2015). Kinetic models in natural sciences. In *Evolutionary Equations with Applications in Natural Sciences* (pp. 133-198). Springer International Publishing.
- [15] Wattis, J. A. (2006). An introduction to mathematical models of coagulation–fragmentation processes: a discrete deterministic mean-field approach. *Physica D: Nonlinear Phenomena*, 222(1), 1-20.
- [16] Bak, P., Tang, C., & Wiesenfeld, K. (1987). Self-organized criticality: An explanation of the $1/f$ noise. *Physical review letters*, 59(4), 381.
- [17] Faybishenko, B., Benson, S. M., Gale, J. E., & Molz, F. (2015). A Complex Systems Approach to Describing Flow and Transport in Fractured-Porous Media. *Fluid Dynamics in Complex Fractured-Porous Systems*, 7(5).
- [18] Lomnitz-Adler, J. (1993). Automaton models of seismic fracture: constraints imposed by the magnitude-frequency relation. *Journal of Geophysical Research: Solid Earth*, 98(B10), 17745-17756.
- [19] Marković, D., & Gros, C. (2014). Power laws and self-organized criticality in theory and nature. *Physics Reports*, 536(2), 41-74.
- [20] Krapivsky, P. L., Redner, S., & Ben-Naim, E. (2010). *A kinetic view of statistical physics*. Cambridge University Press.
- [21] Bodrova, A. S., Stadnichuk, V., Krapivsky, P. L., Schmidt, J., & Brilliantov, N. V. (2019). Kinetic regimes in aggregating systems with spontaneous and collisional fragmentation. *Journal of Physics A: Mathematical and Theoretical*, 52(20), 205001.
- [22] Brilliantov, N., Krapivsky, P. L., Bodrova, A., Spahn, F., Hayakawa, H., Stadnichuk, V., & Schmidt, J. (2015). Size distribution of particles in Saturn’s rings from aggregation and fragmentation. *Proceedings of the National Academy of Sciences*, 112(31), 9536-9541.

- [23] Timokhin, I. V., Matveev, S. A., Siddharth, N., Tyrtysnikov, E. E., Smirnov, A. P., & Brilliantov, N. V. (2019). Newton method for stationary and quasi-stationary problems for Smoluchowski-type equations. *Journal of Computational Physics*, 382, 124-137.
- [24] Kaur, G., Singh, R., Singh, M., Kumar, J., & Matsoukas, T. (2019). Analytical approach for solving population balances: A homotopy perturbation method. *Journal of Physics A: Mathematical and Theoretical*, 52(38), 385201.
- [25] Osinsky, A. I. (2020). Low-rank method for fast solution of generalized Smoluchowski equations. *Journal of Computational Physics*, 422, 109764.
- [26] Smirnov, A. P., Matveev, S. A., Zheltkov, D. A., & Tyrtysnikov, E. E. (2016). Fast and accurate finite-difference method solving multicomponent Smoluchowski coagulation equation with source and sink terms.
- [27] Minh Pham, T., Kondor, I., Hanel, R., & Thurner, S. (2020). The effect of social balance on social fragmentation. *Journal of the Royal Society Interface*, 17(172), 20200752.
- [28] Krapivsky, P. L., Redner, S., & Leyvraz, F. (2000). Connectivity of growing random networks. *Physical review letters*, 85(21), 4629.
- [29] Antal, T., Krapivsky, P. L., & Redner, S. (2005). Dynamics of social balance on networks. *Physical Review E*, 72(3), 036121.
- [30] Barabási, A. L., & Albert, R. (1999). Emergence of scaling in random networks. *science*, 286(5439), 509-512.
- [31] Böhme, G. A., & Gross, T. (2011). Analytical calculation of fragmentation transitions in adaptive networks. *Physical Review E*, 83(3), 035101.
- [32] Almaguer, F. J., Alcalá, M., Berrones, A., Chacón-Mondragón, Ó. L., & Soto-Regalado, E. (2013). Conceptual model of coalescence and break-up in the presence of external agitation. *Physica A: Statistical Mechanics and its Applications*, 392(8), 1725-1732.
- [33] Benavides, L., ALMAGUER, F. J., SCHAEFFER, E., & BERRONES, A. (2018). A Cellular Automaton Model of a Wastewater Treatment Process. *Journal of Cellular Automata*, 13.



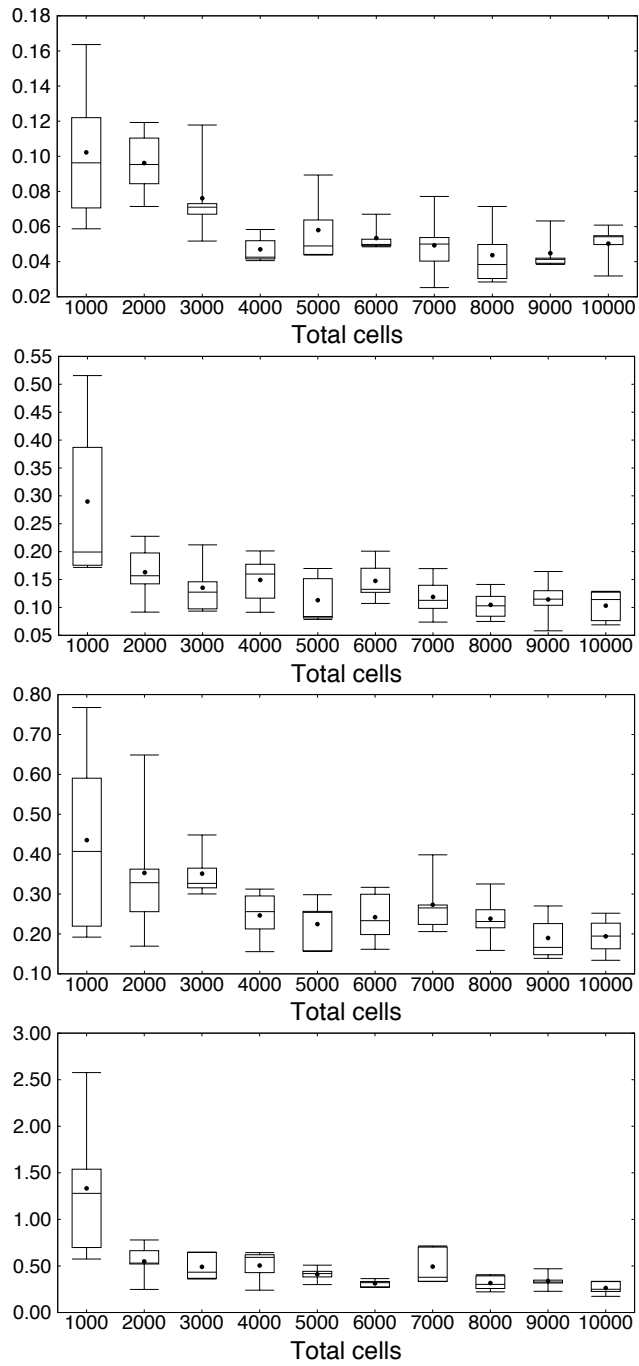


Figure 3: Variance of the same setup as in Figure 2.

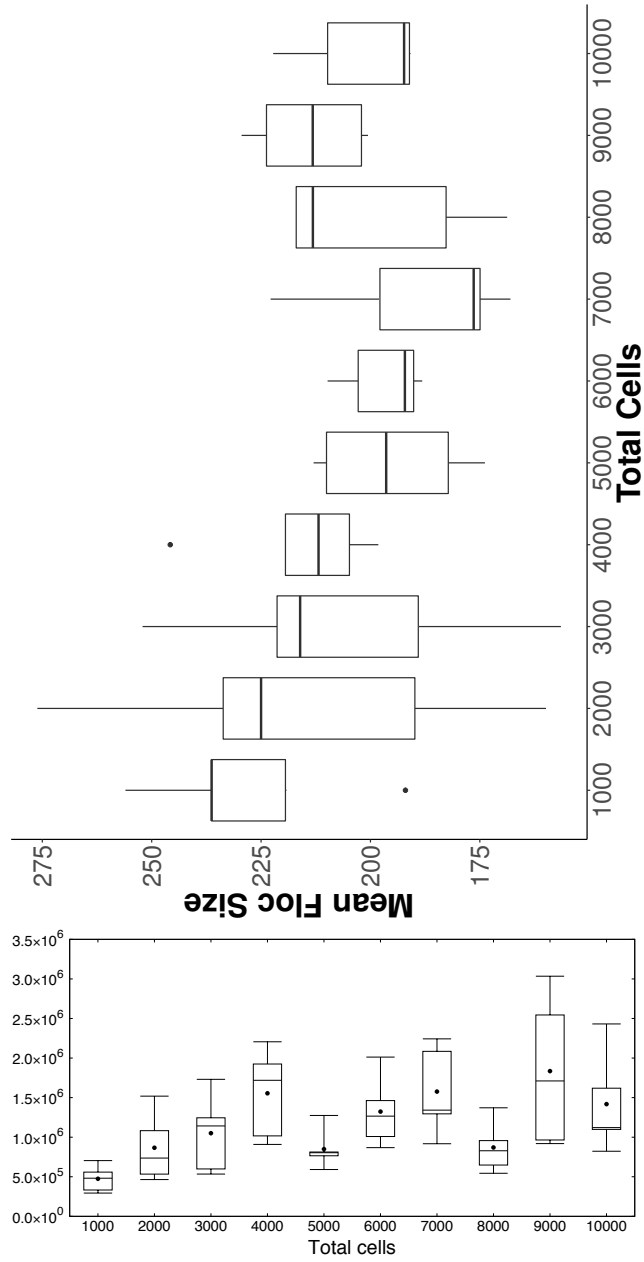
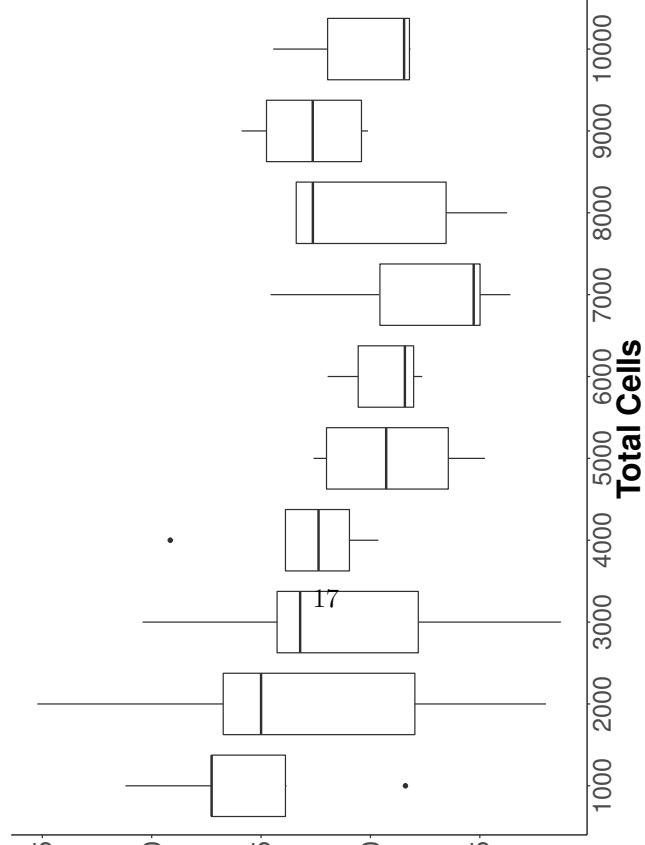
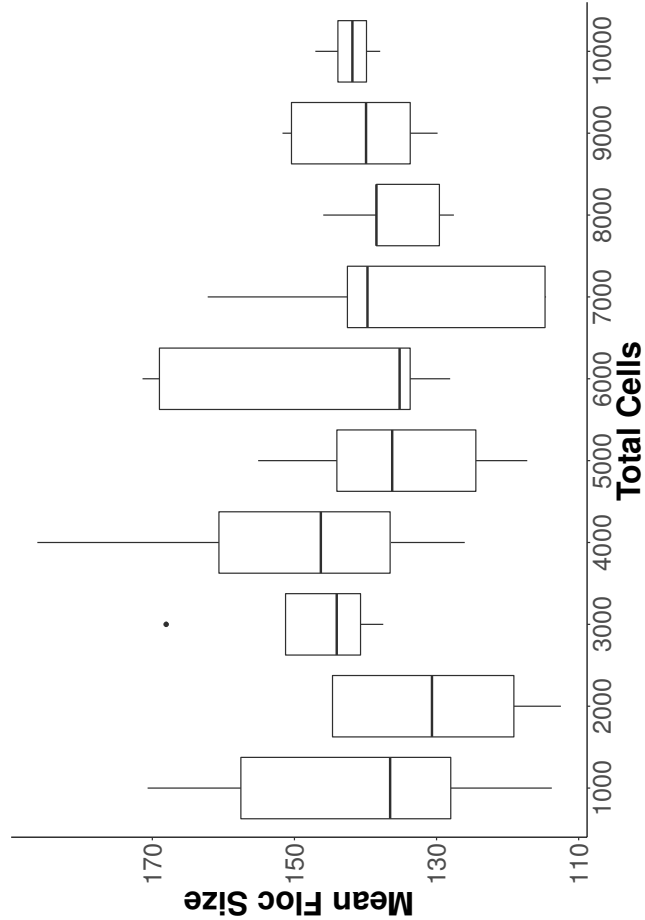


Figure 4: A stationary state with large mean and variance relative to $\bar{h} = 3$ is reported for $f = 0.9$, $v = 0.1$. This is a gel-like state.



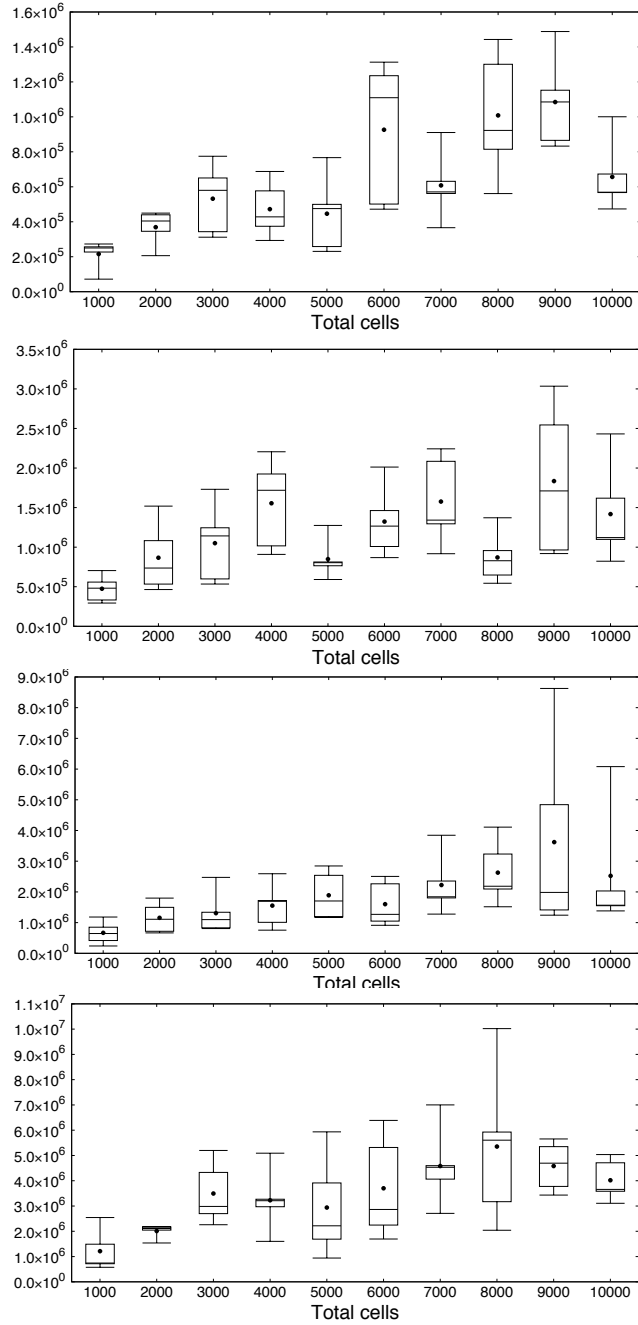


Figure 6: Variance of the same setup as in Figure 5.